Structure and Nonrigidity of $B_{10}H_{11}^-$. An ab Initio/IGLO/NMR Study

Alexander M. Mebel,† Oleg P. Charkin,† Michael Bühl,‡ and Paul von Ragué Schleyer*,‡

Institute of New Chemical Problems, Russian Academy of Sciences, Chernogolovka, Moscow region, 142432 Russia, and Institut für Organische Chemie der Universität Erlangen-Nürnberg, Henkestrasse 42, D-8520 Erlangen, Germany

Received February 12, 1992

Ab initio calculations on $B_{10}H_{11}^-$, i.e. protonated $B_{10}H_{10}^{2-}$, at the MP2/6-31G*//HF/3-21G+ZPE(3-21G) level suggest that the "additional", polycoordinate proton (designated H*) lies above a triangular face in the "polar region" near B1. The marked lengthening (to 2.00 Å) of one of the basal B–B bonds due to coordination with the additional proton in $B_{10}H_{11}^-$ is noteworthy. The structure with a H* doubly bridging above a polar BB edge is the transition state for hydrogen migration around the polar region. This process has an extremely low barrier, ~2 kcal/mol, but bridge/terminal H exchange proceeding via a transition structure with a terminal BH_2 group also is facile (barrier ~8 kcal/mol). However, the transfer of the extra hydrogen from one pole to the other requires greater activation (~19 kcal/mol). These results are in general agreement with the experimental observations. In particular, the calculated IGLO chemical shifts agree with the available experimental data provided that a hydrogen can migrate easily around the 4-fold axis in the polar region.

Introduction

Protonation of *closo*-borane dianions $B_nH_n^{2-}$ leads to new anions of the $B_nH_{n+1}^-$ type with interesting, flexible structures studied experimentally[1,2] and theoretically.[3] While *structural nonrigidity* is well-known in some *closo*-boranes and carboranes,[4-8] the fluxionality of many common boron hydrides is due to rapid hydrogen migrations.[9] In this context, we now report ab initio MO calculations for $B_{10}H_{11}^-$. Our objective is to resolve experimental inconsistencies regarding the molecular structure and to provide details concerning the dynamic behavior.

$B_{10}H_{11}^-$ was synthesized[1] by protonation of $B_{10}H_{10}^{2-}$, which is known to have a bicapped square antiprismatic structure (Figure 1a).[10] The ^{11}B NMR spectrum of $B_{10}H_{11}^-$ at 183 K consists of three signals in a 1:4:5 ratio.[10] Since no reasonable static structure corresponds to this spectrum, a rapid movement of the "additional" (polycoordinate) proton, designated H*, around the "polar cap" B1 (Figure 1b) was suggested to take place. This would result in effective C_{4v} symmetry on the NMR time scale. It was assumed that the B1 and B2–B5 signals could not be resolved; hence, the intensity ratio was not the expected 1:4:4:1. At higher temperatures, the ^{11}B three signals coalesce and merge into a single resonance. This behavior was ascribed to the rapid exchange of the "extra" hydrogen atom H* between the "polar regions" (around B1 and B10) by migration over the "equatorial belt".[2,10] A DNMR barrier of 13 ± 1.5 kcal/mol was deduced for this process.[10]

Earlier quantum chemical calculations at the STO-3G//MNDO and LP-31G//MNDO levels[11] (i.e., ab initio single points using MNDO geometries) were in qualitative agreement with these results. A structure with the extra H* bridging the B1B2B3 face (cf. t455, Figure 2) was found to be the most stable. Scrambling around B1 was predicted to occur via terminal/bridge H exchange (transition structure v4, Figure 2) rather than by the migration over a BB edge (e.g. b45), which is observed e.g. in CB_5H_7[9] and $B_6H_7^-$.[1-3]

The X-ray structure determinations apparently reveal quite different geometries for $B_{10}H_{11}^-$ as a function of the counterions (Ph_3PEt^+ and PPh_4^+).[2] Several elongated B···B separations around 2.11–2.38 Å were found. However, the bridging hydrogen could not be located, and the anion is disordered. As a common geometric model, a structure with only one elongated B···B distance (i.e. with one tetragonal face) was suggested.[2]

Our objective was to determine the ground-state structure of $B_{10}H_{11}^-$ and the transition states connecting possible isomers. We provide additional information by IGLO chemical shift calculations. The ab initio/IGLO[12]/NMR method[13,14] has been

† Russian Academy of Sciences.
‡ Institut für Organische Chemie der Universität Erlangen-Nürnberg.

(1) (a) Wagner, P. A.; Adams, D. M.; Callabretta, F. G.; Spada, L. T.; Unger, R. G. *J. Am. Chem. Soc.* **1973**, *22*, 7513. (b) Vinitskii, D. M.; Lagun, V. L.; Solntsev, K. A.; Kuznetsov, N. T.; Kuznetsov, I. Yu. *Koord. Khim.* **1985**, *11*, 1504 (in Russian). (c) Privalov, V. I.; Tarasov, V. P.; Meladze, M. A.; Vinitskii, D. M.; Solntsev, K. A.; Buslaev, Yu. A.; Kuznetsov, N. T. *Russ. J. Inorg. Chem. (Engl. Transl.)* **1986**, *31* (5), 633.
(2) Kuznetsov, N. T.; Solntsev, K. A. In *Chemistry of Inorganic Hydrides*; Nauka Publ.: Moscow, 1990; p 5 (in Russian).
(3) (a) Mebel, A. M.; Charkin, O. P.; Kuznetsov, I. Yu.; Solntsev, K. A.; Kuznetsov, N. T. *Russ. J. Inorg. Chem. (Engl. Transl.)* **1988**, *33*, 958. (b) Mebel, A. M.; Charkin, O. P.; Solntsev, K. A.; Kuznetsov, N. T. *Russ. J. Inorg. Chem. (Engl. Transl.)* **1989**, *34*, 156; **1989**, *34*, 808; **1989**, *34*, 813. (c) Mebel, A. M.; Charkin, O. P. In *Chemistry of Inorganic Hydrides*; Nauka Publ.: Moscow, 1990; p 43 (in Russian).
(4) (a) Muetterties, E. L.; Wiersema, R. J.; Hawthorne, M. F. *J. Am. Chem. Soc.* **1973**, *95*, 7520. (b) Muetterties, E. L. *Tetrahedron* **1974**, *30*, 1595. (c) Muetterties, E. L.; Hoel, E. L.; Salentine, C. G.; Hawthorne, M. F. *Inorg. Chem.* **1975**, *14*, 950. (d) Kleier, D. A.; Lipscomb, W. N. *Inorg. Chem.* **1979**, *18*, 1312.
(5) (a) Tolpin, E. I.; Lipscomb, W. N. *J. Am. Chem. Soc.* **1973**, *95*, 2384. (b) Kleier, D. A.; Dixon, D. A.; Lipscomb, W. N. *Inorg. Chem.* **1978**, *17*, 166.
(6) (a) Wales, D. J.; Stone, A. J. *Inorg. Chem.* **1987**, *26*, 3845. (b) Wales, D. J.; Mingos, D. M. P.; Zhenyang, L. *Inorg. Chem.* **1989**, *28*, 2754. (c) Mingos, D. M. P.; Wales, D. J. In *Electron Deficient Boron and Carbon Clusters*; Olah, G. A., Wade, K., Williams, R. E., Eds.; Wiley: New York, 1991; Chapter 5, p 143.
(7) (a) Ott, J. J.; Brown, C. A.; Gimarc, B. M. *Inorg. Chem.* **1989**, *28*, 4269. (b) Gimarc, B. M.; Ott, J. J. *Main Group Met. Chem.* **1989**, *12*, 77. (c) Gimarc, B. M.; Daj, B.; Warren, D. S.; Ott, J. J. *J. Am. Chem. Soc.* **1990**, *112*, 2597.
(8) (a) Gaines, D. F.; Coons, D. E.; Heppert, J. A. In *Advances in Boron and Boranes*; Liebmann, F. F., Greenberg, A., Williams, R. E., Eds.; VCH Publishers: Weinheim, New York, 1988; Chapter 5, p 91. (b) Edvenson, G. M.; Gaines, D. F. *Inorg. Chem.* **1990**, *29*, 1210.
(9) (a) Groszek, E.; Leach, J. B.; Wong, J. T. F.; Ungermann, C.; Onak, T. *Inorg. Chem.* **1971**, *10*, 2770. (b) McKee, M. L. *J. Phys. Chem.* **1989**, *93*, 3426. (c) Mebel, A. M.; Charkin, O. P. *Russ. J. Inorg. Chem.* **1990**, *35*, 174 (translated from *Zh. Neorg. Khim.* **1990**, *35*, 312].
(10) Mustyatsa, V. N.; Votinova, N. A.; Solntsev, K. A.; Kuznetsov, N. T. *Dokl. Chem. Proc. Sov. Acad. Sci. (Engl. Transl.)* **1988**, *301*, 245.
(11) Mebel, A. M.; Charkin, O. P.; Solntsev, K. A.; Kuznetsov, N. T. *Russ. J. Inorg. Chem. (Engl. Transl.)* **1988**, *33*, 1292. The calculations were performed with minimal STO-3G and special split-valence LP-31G basis sets for ab initio calculations employing pseudopotentials used in the Gaussian 80 program package.
(12) (a) Kutzelnigg, W. *Isr. J. Chem.* **1980**, *19*, 193. (b) Schindler, M.; Kutzelnigg, W. *J. Chem. Phys.* **1982**, *76*, 1919. Review: (c) Kutzelnigg, W.; Fleischer, U.; Schindler, M. In *NMR, Basic Principles and Progress*; Springer Verlag: Berlin, 1990; p 165.

0020-1669/93/1332-0463$04.00/0

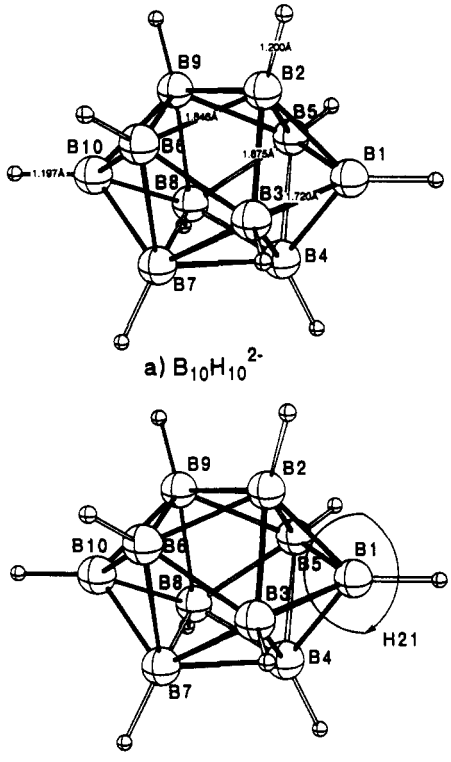

Figure 1. 3-21G-optimized geometry for $B_{10}H_{10}^{2-}$ and geometry for $B_{10}H_{11}^{-}$ assumed from NMR ^{11}B spectrum.

successfully applied to the structural elucidation of electron-deficient boron compounds[13] (as well as carbocations).[14]

Methods

The geometries were fully optimized by employing standard procedures[15] and a 3-21G basis set.[16] In addition, the geometry of the global minimum was reoptimized by employing a 6-31G* basis set[16] at the HF and correlated MP2[17] levels. The Gaussian 90[18] and CADPAC[19] program packages were used. Single point calculations were performed at the correlated MP2/6-31G* level, with the frozen core approximation (notation MP2/6-31G*//3-21G). The nature of each stationary point was probed by analytical frequency calculations at the SCF/3-21G level; transition structures have one and minima have zero imaginary frequencies.

Chemical shifts were calculated using the IGLO (individual gauge for localized orbitals) method.[12] A DZ Huzinaga basis[20] set was used which was contracted as follows: B 7s3p [4111,21], H 3s [21] (notations DZ//3-21G as well as DZ//6-31G* and DZ//MP2/6-31G* for the global minimum).

Results

Geometries. Several alternative geometrical configurations of $B_{10}H_{11}^{-}$ (**1–7**) were considered (Figure 2). Those differ mainly in the position of the critical bridging hydrogen atom: our notation employs "t" to denote a tridentate capping position, "b" to denote a bidentate bridge, and "v" to indicate involvement in a terminal BH_2 group. The numbers 4 and 5 in the notation correspond to the skeletal coordination numbers of the boron atoms that interact with H*. The absolute and relative energies for **1–7** at various levels of theory are summarized in Table I. The optimized geometries are shown in Figure 2.

In the previous calculations[11] the C_s symmetric t455 configuration (**1**) with H* over the B1B2B3 face was the most favorable structure. At the HF/3-21g level, **1** has a very small imaginary frequency (–39 cm^{-1}) and corresponds to a transition state. Reduction of the symmetry to C_1 led to the t455′ minimum (**1′**); however, **1′** was only 0.01 kcal/mol more stable than symmetrical **1**. This part of the PES is extremely flat. At our highest level, MP2/6-31G*//3-21G+ZPE, **1** is again slightly favored (by 0.7 kcal/mol) over **1′**. Only one other local minimum was found, t555 (**2**), with the extra H* capping the equatorial B2B3B6 face, but this was 15.0 kcal/mol less stable than **1** (MP2/6-31G*//3-21G+ZPE).

Protonation of $B_{10}H_{10}^{2-}$ changes the structure of the boron skeleton significantly. The most dramatic deformation of $B_{10}H_{11}^{-}$ (**1**) is the lengthening of the B2–B3 edge bond involved in the critical hydrogen bridge (to 2.14 Å at the SCF/3-21G level; Figure 2). However, this bond is not fully broken: the Wiberg bond index[21] (WBI) is 0.26 (Table II). The other bridged B1B2 and B1B3 distances also increase significantly in going to $B_{10}H_{11}^{-}$. The nearest edges of the pyramid base (B2B5 and B3B4 in **1**) are shortened by 0.06 Å (SCF/3-21G), but the other BB bond lengths change less than ca. 0.02–0.03 Å. Deviations of the BBB bond angles are less pronounced and do not exceed ca. 2–3°, except for the B2B1B3 and B2B6B3 angles "opposite" the long B2B3 bond. These angles increase by 4 and 9°, respectively.

Reoptimization of the 3-21G geometry of **1** employing the MP2/6-31G* approximation led to a shortening of the bridged B2B3 and B1B2, B1B3 bonds by 0.14 (to 2.00 Å) and 0.07 Å, respectively (see Figure 2). Also, the B2H* and B3H* distances are diminished by 0.05 Å. Nevertheless, most of the conclusions concerning deformation of the boron skeleton due to protonation remain valid.

The four boron atoms, B1, B2, B3, and B6, do not constitute a square open face. Rather, they form a "butterfly" arrangement (local D_{2d} symmetry) with a "hinge" dihedral angle of 156.7° (cf. the corresponding 153.7° value in $B_{10}H_{10}^{2-}$). The four-center hydrogen bridge is somewhat unsymmetrical: the hydrogen is more strongly bound to B1 (B1–H* = 1.28 Å) than to B2 and B3 (B(2,3)–H* = 1.48 Å). This difference is also reflected in the Wiberg bond index: 0.47 for B1–H* and 0.21 for the B(2,3)–H* bonds in the t455 configuration. The bonds involving the triply bridged hydrogen to each boron are weaker than the bonds involving terminal hydrogens. The range of terminal BH distances is 1.18–1.19 Å; the Wiberg indices are 0.95–0.96.

(13) (a) Schleyer, P. v. R.; Bühl, M.; Fleischer, U.; Koch, W. *Inorg. Chem.* **1990**, *29*, 153. (b) Bühl, M.; Schleyer, P. v. R. *Angew. Chem., Int. Ed. Engl.* **1990**, *29*, 886. (c) Bühl, M.; Schleyer, P. v. R. In *Electron Deficient Boron and Carbon Clusters*; Olah, G. A., Wade, K., Williams, R. E., Eds.; Wiley: New York, 1990; Chapter 4, p 113. (d) Bühl, M.; Schleyer, P. v. R.; McKee, M. L. *Heteroatom Chem.* **1991**, *2*, 499. (e) Bühl, M.; Schleyer, P. v. R. *J. Am. Chem. Soc.* **1992**, *114*, 477.

(14) (a) Schindler, M. *J. Am. Chem. Soc.* **1987**, *109*, 1020. (b) Bremer, M.; Schleyer, P. v. R.; Schötz, K.; Kausch, M.; Schindler, M. *Angew. Chem.* **1987**, *99*, 795. (c) Schleyer, P. v. R.; Laidig, K. E.; Wiberg, K. B.; Saunders, M.; Schindler, M. *J. Am. Chem. Soc.* **1988**, *110*, 300. (d) Saunders, M.; Laidig, K. E.; Wiberg, K. B.; Schleyer, P. v. R. *J. Am. Chem. Soc.* **1988**, *110*, 7652. (e) Schleyer, P. v. R.; Carneiro, J. W. d. M.; Koch, W.; Raghavachari, K. *J. Am. Chem. Soc.* **1989**, *111*, 5475. (f) Bremer, M.; Schleyer, P. v. R.; Fleischer, U. *J. Am. Chem. Soc.* **1989**, *111*, 1147. (g) Bremer, M.; Schötz, K.; Schleyer, P. v. R.; Fleischer, U.; Schindler, M.; Kutzelnigg, W.; Pulay, P. *Angew. Chem.* **1989**, *101*, 1063. (h) Schleyer, P. v. R.; Koch, W.; Liu, B.; Fleischer, U. *J. Chem. Soc., Chem. Commun.* **1989**, 1098. (i) Schleyer, P. v. R.; Carneiro, J. W. d. M. *J. Am. Chem. Soc.* **1990**, *112*, 4046.

(15) Hehre, W.; Radom, L.; Schleyer, P. v. R.; Pople, J. A. *Ab Initio Molecular Orbital Theory*; Wiley: New York, 1986.

(16) (a) 3-21G: Binkley, J. S.; Pople, J. A.; Hehre, W. J. *J. Am. Chem. Soc.* **1980**, *102*, 939. (b) Gordon, M. S.; Binkley, J. A.; Pople, J. A.; Petro, W. J.; Hehre, W. J. *J. Am. Chem. Soc.* **1982**, *104*, 2797. 6-31G*: (c) Hariharan, P. C.; Pople, J. A. *Theor. Chim. Acta* **1973**, *28*, 213. (d) Francl, M. M.; Peitro, W. J.; Hehre, W. J.; Binkley, J. S.; Gordon, M. S.; DeFrees, D. J.; Pople, J. A. *J. Chem. Phys.* **1982**, *77*, 3654.

(17) Binkley, J. S.; Pople, J. A. *Int. J. Quantum Chem.* **1975**, *9*, 229 and references therein.

(18) Gaussian 90: Frisch, M. J.; Head-Gordon, M.; Trucks, G. W.; Foresman, J. B.; Schlegel, H. B.; Raghavachari, K.; Robb, M. A.; Binkley, J. S.; Gonzales, C.; DeFrees, D. J.; Fox, D. J.; Whiteside, R. A.; Seeger, R.; Melius, C. F.; Baker, J.; Martin, R. L.; Kahn, L. R.; Stewart, J. J. P.; Topiol, S.; Pople, J. A. Gaussian Inc., Pittsburg, PA, 1990.

(19) Amos, R. D.; Rice, J. E. CADPAC: *The Cambridge Analytical Derivatives Package*, Issue 4.0. Cambridge, 1987.

(20) Huzinaga, S. *Approximate Atomic Wave Functions*; University of Alberta: Edmonton, Canada, 1971.

(21) Wiberg, K. B. *Tetrahedron* **1968**, *24*, 1083.

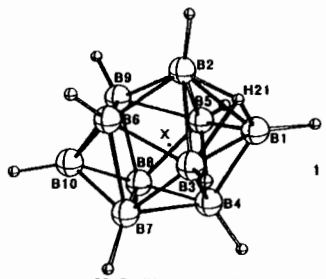

1

t455, C_s (H on face B_4-B_5-B_5)

Interatomic distances(Å):

B1-B2	[illegible]	B2-H21	1.542(1.483)
B2-B3	[illegible]	B1-H21	1.280(1.282)
B1-B4	[illegible]	B2-H	1.184(1.189)
B3-B4	[illegible]	B4-H	1.188(1.192)
B2-B6	[illegible]	B8-H	1.188(1.193)
B3-B7	[illegible]	B7-H	1.188(1.193)
B4-B5	[illegible]	B6-H	1.190(1.195)
B4-B7	[illegible]	B1-H	1.181(1.186)
B4-B8	[illegible]	B10-H	1.184(1.190)
B6-B7	[illegible]		
B7-B8	[illegible]		
B8-B10	[illegible]		
B7-B10	[illegible]		
B5-B10	[illegible]		

Bond angles (degrees):

B3-B1-B2	69.9(69.0)		
B3-B1-B4	60.5(60.9)		
B4-B1-B5	66.7(66.4)		
B3-B2-B1	55.1(55.5)		
B4-B3-B1	56.0(56.4)		
B3-B4-B1	63.5(62.7)		
B3-B6-B2	69.9(67.9)		
B3-B2-B6	55.1(56.1)		
B1-H21-B2	82.3(82.6)		
B2-H21-B3	87.8(88.7)		
X-B2-H	177.6(177.0)		
X-B4-H	177.5(177.1)		
X-B8-H	171.5(170.1)		
X-B7-H	174.3(173.7)		
X-B6-H	175.2(173.6)		
X-B1-H	172.0(174.0)		
X-B10-H	178.9(178.9)		

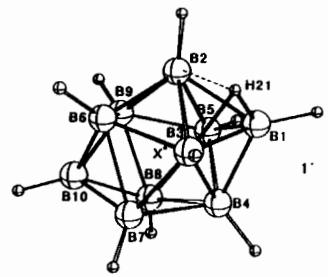

1'

t455', C_1 (H on face B_4-B_5-B_5)

Interatomic distances(Å):

B1-B3	1.837	B1-H21	1.276
B1-B2	1.898	B3-H21	1.437
B1-B4	1.732	B2-H21	1.722
B1-B5	1.738	B3-H	1.186
B2-B3	2.141	B2-H	1.183
B3-B4	1.836	B4-H	1.188
B2-B5	1.799	B5-H	1.187
B4-B5	1.907	B8-H	1.188
B3-B6	1.884	B7-H	1.188
B2-B6	1.842	B5-H	1.189
B2-B9	1.808	B6-H	1.190
B5-B9	1.828	B1-H	1.182
B5-B8	1.839	B10-H	1.184
B4-B8	1.837		
B4-B7	1.811		
B1-B8	1.855		
B8-B10	1.737		
B7-B10	1.695		
B5-B10	1.700		
B6-B10	1.737		
B7-B8	1.834		
B8-B9	1.850		
B6-B7	1.929		
B6-B9	1.886		

Bond angles (degrees):

B3-B1-B2	69.9	X-B3-H	171.6
B3-B1-B4	61.8	X-B2-H	177.5
B2-B1-B5	59.1	X-B4-H	176.7
B4-B1-B5	66.7	X-B5-H	176.9
B3-B2-B1	53.7	X-B8-H	173.3
B2-B3-B1	56.4	X-B7-H	174.6
B4-B3-B1	56.3	X-B9-H	172.1
B2-B5-B1	64.9	X-B6-H	173.4
B3-B6-B2	70.1	X-B1-H	173.5
B3-B2-B6	55.9	X-B10-H	178.7
B2-B3-B6	54.0	B1-H21-B3	85.0
B9-B2-B6	62.2	B1-H21-B2	77.0
B8-B10-B7	64.6	B3-H21-B2	84.8

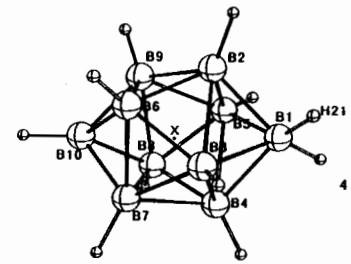

4

v4, C_{2v} (BH_2-group with B_4-atom)

Interatomic distances(Å):

B1-B2	1.839	B1-H21	1.196
B2-B3	2.080	B2-H	1.185
B3-B4	1.750	B6-H	1.189
B3-B7	1.819	B7-H	1.189
B8-B10	1.775	B1-H	1.196
B7-B10	1.685	B10-H	1.184
B6-B7	1.886		
B3-B6	1.826		

Bond angles (degrees):

B2-B1-B3	68.9	X-B1-H	127.6
B3-B1-B4	56.8	X-B2-H	171.8
B2-B3-B1	55.6	X-B6-H	163.3
B3-B4-B1	61.6	X-B7-H	162.0
B2-B3-B6	55.3	X-B10-H	180.0
B2-B6-B3	69.4		
B7-B8-B10	54.7		

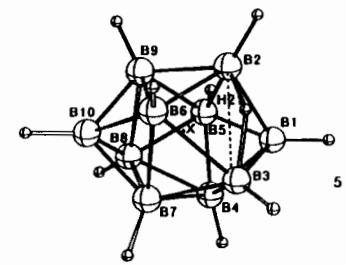

5

b55, C_s (H on edge B_5-B_5)

Interatomic distances(Å):

B2-B3	2.356	B2-H21	1.383
B1-B2	1.846	B1-H21	1.921
B2-B6	2.111	B6-H21	1.747
B3-B4	1.812	B2-H	1.184
B3-B7	1.764	B1-H	1.181
B1-B4	1.702	B6-H	1.183
B4-B5	1.811	B4-H	1.187
B6-B7	1.874	B7-H	1.188
B4-B7	1.893	B8-H	1.189
B4-B8	1.835	B10-H	1.183
B7-B8	1.888		
B6-B10	1.683		
B7-B10	1.732		
B8-B10	1.700		

Bond angles (degrees):

B2-B1-B3	79.2	X-B2-H	179.8
B1-B2-B3	50.4	X-B4-H	171.2
B2-B6-B3	67.8	X-B8-H	171.9
B6-B2-B3	67.8	X-B7-H	178.9
B3-B1-B4	61.3	X-B6-H	164.0
B1-B4-B3	63.3	X-B1-H	176.2
B3-B6-B7	52.1	X-B10-H	177.5
B3-B7-B6	70.9	B2-H21-B3	116.7
B7-B3-B4	63.9		
B3-B4-B7	56.8		

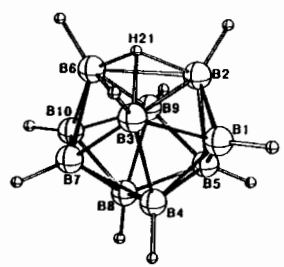

2

t555, C_s (H on face B_5-B_5-B_5)

Interatomic distances(Å):

B1-B2	1.740	B6-H21	1.311
B1-B4	1.730	B2-H21	1.514
B2-B3	2.190	B2-H	1.184
B3-B4	1.832	B4-H	1.187
B4-B5	1.820	B8-H	1.189
B2-B6	2.128	B7-H	1.188
B4-B8	1.814	B6-H	1.187
B4-B7	1.862	B1-H	1.185
B3-B7	1.848	B10-H	1.182
B8-B10	1.896		
B7-B10	1.727		
B6-B10	1.698		
B7-B8	1.883		
B6-B7	1.914		

Bond angles (degrees):

B2-B6-B3	61.9	X-B2-H	177.6
B2-B3-B6	59.0	X-B4-H	170.6
B2-B1-B3	78.0	X-B8-H	173.6
B2-B3-B1	51.0	X-B7-H	179.6
B3-B1-B4	62.6	X-B6-H	175.5
B4-B1-B3	56.9	X-B1-H	177.6
B3-B4-B1	60.5	X-B10-H	177.9
B4-B1-B5	63.4	B2-H21-B3	92.6
B4-B5-B1	58.3	B2-H21-B6	97.5
B2-B6-B9	54.1		
B6-B7-B3	68.9		

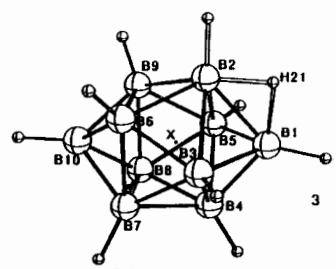

3

b45, C_s (H on edge B_4-B_5)

Interatomic distances(Å):

B1-B2	1.796	B2-H21	1.300
B1-B3	1.806	B1-H21	1.300
B1-B4	1.748	B2-H	1.193
B2-B3	1.984	B3-H	1.188
B3-B4	1.839	B4-H	1.186
B2-B6	1.895	B7-H	1.189
B3-B6	1.788	B6-H	1.188
B3-B7	1.802	B1-H	1.184
B4-B7	1.818	B10-H	1.185
B6-B9	2.036		
B6-B7	1.832		
B7-B8	1.876		
B7-B10	1.732		
B6-B10	1.715		

Bond angles (degrees):

[illegible]	66.8	X-B2-H	155.6
[illegible]	62.3	X-B3-H	178.5
[illegible]	56.8	X-B4-H	179.7
[illegible]	60.4	X-B7-H	175.2
[illegible]	65.0	X-B6-H	179.3
[illegible]	57.5	X-B1-H	168.0
[illegible]	54.8	X-B10-H	177.7
[illegible]	65.2	B1-H21-B2	87.4
[illegible]	53.6		
[illegible]	72.8		

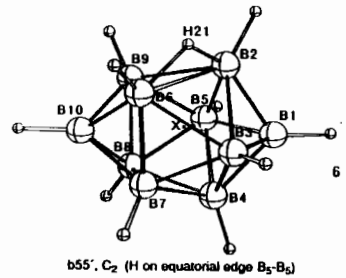

6

b55', C_2 (H on equatorial edge B_5-B_5)

Interatomic distances(Å):

B1-B3	1.684	B2-H21	1.314
B1-B2	1.719	B3-H	1.187
B1-B4	1.711	B2-H	1.189
B1-B5	1.769	B3-H	1.188
B2-B3	2.074	B5-H	1.189
B3-B4	1.868	B1-H	1.184
B2-B5	1.834		
B4-B5	1.855		
B3-B6	2.051		
B2-B6	2.119		
B5-B8	1.844		
B4-B8	1.807		
B3-B7	1.808		

Bond angles (degrees):

B3-B6-B2	59.6	X-B3-H	165.1
B3-B2-B6	58.6	X-B2-H	173.8
B3-B7-B7	68.5	X-B4-H	169.6
B3-B2-B1	51.7	X-B5-H	171.7
B2-B3-B1	53.2	X-B1-H	174.0
B3-B1-B2	75.1	B2-H21-B6	107.5
B2-B1-B5	63.4		
B3-B1-B4	66.7		
B4-B1-B5	64.4		

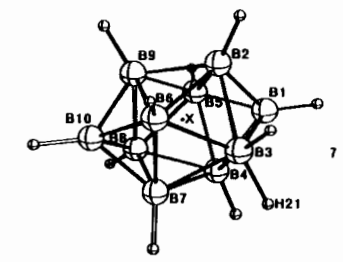

7

v5, C_s (BH_2-group with B_5 atom)

Interatomic distances (Å):

B2-B3	1.958	B3-H21	1.210
B3-B7	1.894	B3-H	1.210
B1-B3	1.851	B1-H	1.185
B1-B2	1.715	B2-H	1.183
B1-B5	1.694	B5-H	1.187
B2-B6	2.070	B8-H	1.190
B2-B5	1.863	B7-H	1.184
B7-B6	1.882	B10-H	1.183
B6-B7	1.762		
B2-B9	1.807		
B5-B8	1.871		
B8-B9	1.890		
B7-B10	1.715		
B8-B10	1.709		

Bond angles (degrees):

B2-B3-B1	53.4	X-B3-H	133.9
B3-B2-B1	60.1	X-B2-H	162.3
B3-B1-B2	66.5	X-B5-H	166.1
B6-B3-B7	55.4	X-B8-H	168.1
B3-B6-B7	62.3	X-B7-H	161.0
B2-B3-B6	65.0	X-B1-H	172.1
B3-B2-B6	56.0	X-B10-H	179.3
B2-B6-B9	54.2	X-B3-H21	133.9
B2-B9-B5	68.2	H-B3-H21	91.3

Figure 2. 3-21G-optimized geometries for $B_{10}H_{11}^-$ (1–7). (For **1** in parentheses: 6-31G*-optimized geometry.)

Table I. Absolute (-au) and Relative (kcal/mol, in Brackets) Energies for Different Structures of $B_{10}H_{11}^-$

	level of theory					
struct, sym (no.)	SCF/3-21G	ZPE[a]	SCF/DZ[b]	SCF/6-31G*[b]	MP2/6-31G*[b]	final[c]
t455, C_s (1)	251.815 35 [0.01]	95.2 (1)	252.984 70 [0.03]	253.258 53 [0.0]	254.220 42 [0.0]	[0.0]
t455', C_1 (1')	251.815 36 [0.00]	95.6 (0)	252.984 74 [0.00]	253.258 09 [0.3]	254.219 97 [0.3]	[0.7]
t555, C_s (2)	251.797 92 [10.9]	95.0 (0)	252.968 59 [10.1]	253.238 24 [12.7]	254.196 16 [15.2]	[15.0]
b45, C_s (3)	251.811 91 [2.2]	95.9 (1)	252.982 45 [1.4]	253.253 54 [3.1]	254.217 65 [1.7]	[2.3]
v4, C_{2v} (4)	251.808 09 [4.6]	95.3 (1)	252.978 28 [4.1]	253.243 99 [9.1]	254.207 00 [8.4]	[8.5]
b55, C_s (5)	251.788 25 [17.0]	94.0 (1)	252.957 20 [17.3]	253.228 64 [17.5]	254.189 23 [19.6]	[18.5]
b55', C_2 (6)	251.791 92 [14.7]	94.3 (1)	252.962 92 [13.7]	253.230 89 [17.3]	254.190 01 [19.1]	[18.3]
v5, C_s (7)	251.753 41 [38.9]	92.2 (2)	252.920 26 [42.1]	253.184 50 [46.5]	254.157 72 [39.3]	[36.6]

[a] 3-21G zero-point energy; in parentheses are the number of imaginary frequencies. [b] For 3-21G geometry. [c] MP2/6-31G*//3-21G + ZPE(3-21G), ZPE's scaled by 0.89 as recommended in ref 15.

Table II. Natural Charges and Wiberg Bond Indexes for the $B_{10}H_{11}^-$ Anion (SCF/3-21G)

		$B_{10}H_{11}^-$							
atoms	$B_{10}H_{10}^{2-}$ (D_{4d})	t455, C_s (1)	t455', C_1 (1')	t555, C_s (2)	b45, C_s (3)	v4, C_{2v} (4)	b55, C_s (5)	b55', C_2 (6)	v5, C_s, (7)
				Charges					
B1	-0.27	-0.24	-0.23	-0.30	-0.25	-0.49	-0.10	-0.26	-0.26
B2	-0.15	-0.02	+0.02	+0.02	-0.14	-0.02	-0.07	-0.09	+0.08
B3			-0.05		-0.13			+0.03	-0.71
B4		-0.16	-0.17	-0.12	-0.09		-0.17	-0.11	
B5			-0.16					-0.21	-0.03
B6		-0.17	-0.18	-0.08	-0.08	-0.14	+0.04		-0.01
B7		-0.14	-0.12	-0.16	-0.15	-0.19	-0.19		
B8		-0.11	-0.11	-0.15			-0.13		-0.23
B9			-0.16						
B10		-0.18	-0.18	-0.19	-0.19	-0.11	-0.23		-0.20
H21		+0.21	+0.21	+0.14	+0.24	+0.15	+0.15	+0.16	+0.24
				WBI					
1-2	0.67	0.46	0.45	0.69	0.52	0.50	0.54	0.67	0.56
1-3			0.49		0.58			0.75	0.68
2-3	045	0.26	0.27	0.23	0.39	0.30	0.17	0.33	
3-4		0.53	0.51	0.45	0.48	0.62	0.49	0.42	
2-5			0.55					0.52	0.41
3-6	0.54	0.57	0.56	0.28	0.61	0.59	0.33	0.36	
3-7		0.51	0.48	0.58		0.52	0.66	0.61	0.51
2-6			0.59		0.48			0.32	0.30
4-7		0.54	0.56	0.51			0.46	0.52	
6-10		0.64	0.64	0.66	0.68		0.71		0.64
7-10		0.68	0.69	0.64		0.72	0.61	0.58	
8-10		0.62	0.61	0.66	0.63	0.55	0.68		0.66
1-21		0.47	0.48		0.42	0.82	0.08		
2-21		0.21	0.12	0.23	0.43		0.34	0.43	
3-21			0.29						0.75
6-21				0.45			0.15		
1-11	0.95	0.95	0.95	0.95	0.94	0.82	0.96	0.95	0.95
3-13	0.96	0.96	0.96	0.96	0.92	0.96	0.96	0.96	0.75

In summary, as with previous results,[11] our calculations confirm that the two differently appearing X-ray structures of $B_{10}H_{11}^-$ are artifacts of crystal disorder. The equilibrium geometry of the $B_{10}H_{11}^-$ anion has only one strongly lengthened BB distance. The disordering of this elongated BB distance along the 4-fold axis through B1 and B10 results in the structure shown in Figure 1a. The disordering along a twofold axis passing through the B3B6 and B5B8 equatorial edges affords the configuration shown in Figure 1b.

Nonrigid Behavior. The "extra" hydrogen atom in **1** is situated in the "polar region" over a triangular face involving B1. The b45 form (**3**) represents the transition structure for the migration of this extra hydrogen in **1** or its exchange with some terminal H to give an equivalent minimum on an adjacent polar face. A rapid sequence of such processes renders the equatorial borons B2–B5 and B6–B9 equivalent. This scrambling barrier is computed to be very low, 2.3 kcal/mol (Table I). Hence, the two sets of equatorial borons are expected to be equivalent on the NMR time scale, in agreement with the experimental findings.[10] An alternative scrambling mechanism via bridge/terminal H exchange proceeds through transition structure v4 (**4**), which has a terminal BH_2 group. This process requires only somewhat larger activation, 8.5 kcal/mol. Hence, even at low temperatures, the additional proton is effectively "spread out" over the whole polar region.

The local minimum t555 (**2**) is an intermediate on the minimum energy pathway assumed for the migration of the extra hydrogen from one polyhedron pole to the other. In going from **1** to **2**, the extra H* passes over the B2B3 edge through transition structure b55 (**5**); the barrier is 18.5 kcal/mol. The subsequent passage over an equatorial edge B2B6 [transition structure b55' (**6**)] to an adjacent equatorial face is facile (starting from **2**, the barrier is 3.3 kcal/mol). Finally, the additional proton reaches the face near B10 through a transition state equivalent to b55 (**5**). The highest energy barrier on the whole pathway is 18.5 kcal/mol. This value is somewhat greater than the experimental estimate of 13 ± 1.5 kcal/mol. However, the levels of theory we have employed are not high (in view of the size of the systems). Also, fast exchange of H* with the protic solvent (trifluoroacetic acid in CD_3CN)[10] might be a viable alternative mechanism.

Compared to $B_{10}H_{10}^{2-}$, the additional hydrogen in $B_{10}H_{11}^-$ results in large deformations of the boron skeleton, particularly in the region closest to the extra H*. The bonds between four-coordinated and five-coordinated boron atoms behave differently: the weaker (i.e. longest) B_5–B_5 bonds are elongated to the

Table III. NMR ^{11}B Chemical Shifts (ppm) for the $B_{10}H_{11}^-$ Anion (DZ//3-21G)

	configuration, point group (no.)								
atom	t455, C_s[a] (1)	t455′, C_1 (1′)	t555 C_2 (2)	b45, C_s (3)	v4, C_{2v} (4)	b55, C_s (5)	b55′, C_2 (6)	v5, C_s (7)	expt[b]
B1	−23.5 (−21.9) [−24.7]	−22.3	−12.9	−16.9	−16.9	+3.6	+4.4	+4.6	
B2	−9.8 (−16.4) [−17.9]	−3.0	−18.9	−18.4	+11.9	−24.4	−24.9	+4.5	
B3		−13.6		−21.4			−5.5	−65.3	
B4	−21.0 (−24.5) [−24.1]	−24.7	−10.0	+5.5		−21.4	−6.5		
B5		−15.1					−27.5	+23.9	
B6	−28.7 (−30.2) [−30.6]	−26.7	−29.4	−4.3	+1.3	−20.1		−8.2	
B7	−23.0 (−21.9) [−25.8]	−17.1	−24.0	−25.6	−17.9	−24.4			
B8	−12.2 (−14.4) [−17.9]	−11.5	−22.3			−24.5		−25.0	
B9		−27.3							
B10	+24.9 (+17.9) [+22.2]	+27.3	+19.1	+33.1	+34.4	−0.7	+4.4	+10.4	+25.7 (1B)
(B2–B5)[c]	−15.4 (−20.5) [−21.6]	−14.1	−14.5	−13.9	+11.9	−22.9	−16.1	−8.1	−21.5 (4B)
(B6–B9)[c]	−21.7 (−22.1) [−25.0]	−20.6	−24.9	−15.0	−8.3	−23.4	−16.1	−16.6	
(B1–B5)[c]	−17.0 (−20.9) [−22.2]	−15.7	−14.2	−14.5	+6.1	−17.6	−12.0	−5.5	
(B1, B6–B9)[c]	−22.1 (−22.1) [−24.9]	−20.1	−22.5	−15.4	−13.7	−22.7	−12.0	−15.7	−25.6 (5B)

[a] In parentheses, DZ//6-31G* values; in brackets, DZ//MP2/6-31G* values. [b] Experimental data from refs 2 and 10. Three signals with the 1:4:5 intensity ratio were observed. [c] Averaged values.

largest extent (ca. 0.20–0.30 Å). In the transition structure b55 (**5**), where the additional proton is situated over an B_5–B_5 edge, B2B3 lengthens to 2.36 Å and the WBI is lowered to 0.17. Nevertheless, the tetragonal face which is formed is nonplanar; the (1–2–9,1–2–8) dihedral angle is 158.3° (Figure 2). The equatorial B_5–B_5 bonds are not distorted as much: the largest elongation compared to $B_{10}H_{10}^{2-}$ is observed in the t555 local minimum (0.28 Å). The stronger (and shorter) B_4–B_5 bonds are deformed to a lesser extent.

While the terminal BH bond lengths do not change upon protonation, angular deviations of the terminal hydrogens from the cluster axis XB (where X denotes the center of mass) up to 20–25° are found. The hydrogens attached to the boron atoms which interact with the extra H* usually are bent outward more strongly. For example, in the b45 configuration, the hydrogen atom on the capping B1 is bent by 12° and the hydrogen on B2 by 24.4°. However, the bending of terminal hydrogens on cluster sites farther away from the extra H* also are noticeable; e.g., the B7 and B8 H's in the v4 structure (Figure 2) deviate from the XB axis by 17–18°.

Electronic Structure. The natural charges of the atoms and the Wiberg bond indices obtained as result of the natural population analysis[22] (NPA) for the $B_{10}H_{10}^{2-}$ dianion and the various $B_{10}H_{11}^-$ structures are summarized in Table II. The negative charge (−0.27 e) on the 4-coordinated borons (B1,B10) is significantly larger than the charge (−0.15 e) on the 5-coordinated B_5's. The charges on the various types of hydrogen are all very small (ca. −0.02 to −0.03 e). Hence, the capping boron atoms should be the preferred electrostatically during the protonation of $B_{10}H_{10}^{2-}$. The B_4–H* bridging bond is stronger than that involving B_5–H*. This difference is related to the relative energies of the transition states b45 and b55. In going from t455 to b45, the weaker B_5–H* bond must be broken, whereas, in going from t455 to b55, the stronger B_4–H* bond is cleaved. Consequently, the migration of the additional proton around the pole is more facile than from one pole to the other.

In $B_{10}H_{11}^-$ the bridging hydrogen is more positively charged (+0.21 e) than the terminal hydrogens. The anion electron density is polarized. The greatest decrease in negative charge is found for the B(2,3) atoms facing the extra hydrogen and also for the remote B10 atom. As a result, the maximum negative charge (−0.24 e) in $B_{10}H_{11}^-$ remains on the apical B1 atom which is interacting with H*. The smallest electron density (−0.02 e) is observed on the B2 and B3 atoms.

The WBI values reflect the geometric deformations. The greatest decrease in the WBI is for the most strongly elongated BB bonds. The Wiberg indices for the terminal BH bonds change only slightly.

Chemical Shift Calculations. The IGLO chemical shifts for the various $B_{10}H_{11}$ structures are summarized in Table III. The experimental NMR ^{11}B spectrum consists of three signals at 25.7, −21.5, and −25.6 ppm with a 1:4:5 intensity ratio.[10] For the comparison of experimental and IGLO chemical shifts it is necessary to take the rapid proton migration around a polyhedron pole into account (see above). Therefore, the chemical shifts for B2–B5 and B6–B9 were averaged. The chemical shifts of the 3-21G-optimized t455 structure correspond to the experimental data most closely (Table III). Excellent agreement between calculated and experimental chemical shifts are found for B10 (deviation only −0.8 ppm), B6–B9 (−0.2), and B1 (+2.1). However, the averaged IGLO chemical shift for B2–B5 (−15.4) shows a rather large deviation from the experimental values for the signals with 5-fold (−25.6) and 4-fold (−21.5) intensities. Recalculation of the chemical shifts at the DZ//6-31G* level significantly improved the correspondence of the B2–B5 IGLO value with experiment. Moreover, the chemical shifts computed for B1 and B2–B5 are indicated to be quite similar (−21.9 and −20.5 ppm, respectively), in agreement with the experimental observation of a 5-fold signal. The B6–B9 chemical shift value changes only slightly. However, at that level, the accord of the B10 chemical shift worsened (IGLO, 17.9 ppm; experiment, 25.7 ppm). This is probably due to the sensitivity of this antipodal[23] boron toward perturbations of the opposite cage vertex. Still higher levels of theory are required for a correct description of the B10 chemical shift. Indeed, calculation at the DZ//MP2/6-31G* level gives the antipodal shift value at 22.2 ppm and discrepancy from experiment decreases to 3.5 ppm. The IGLO DZ//MP2/6-31G* chemical shifts for B1 (−24.7) and B6–B9 (−25.0) are very close, and their averaged value (−24.9) differs only by 0.7 ppm from the experimental shift of the 5-fold signal. The IGLO value for B2–B5 (−21.6) is in accord with chemical shift (−21.5 ppm) of the 4-fold NMR ^{11}B signal. Thus, the agreement of the IGLO chemical shifts with experiment is satisfactory.

The IGLO calculations for unsymmetrical t455′ (**1′**) also reproduce the experimental data well (Table III). The calculated values for the other geometries differ from experiment to a greater extent. For the second minimum t555 (**2**), the rapid migration of H* over the equatorial belt (barrier 3.3 kcal/mol) would average the chemical shifts for the B2–B9 and B1, B10 atoms. Since the calculated values, −19.7 and 3.1 ppm, respectively, as well as 4:1 intensity ratio are not in agreement with the experimental findings, isomer **2** can be excluded. Thus, the ab initio/IGLO/NMR calculations confirm the conclusion that the additional hydrogen

(22) Reed, A. E.; Curtiss, L. A.; Weinhold, F. *Chem. Rev.* **1988**, *88*, 899.

(23) Bühl, M.; Schleyer, P. v. R.; Havlas, Z.; Hnyk, D.; Hermanek, S. *Inorg. Chem.* **1991**, *30*, 3107.

Table IV. Calculated IR Wavenumbers[a] and Intensities[b] (3-21G Basis) of the Most Intensive Vibrations for $B_{10}H_{10}^{2-}$ and Different Configurations of $B_{10}H_{11}^{-}$ Anions

	$B_{10}H_{11}^{-}$							
$B_{10}H_{10}^{2-}$ (D_{4d})	t455, C_s (**1**)	t455′, C_1 (**1′**)	t555,, C_s (**2**)	b45, C_s (**3**)	v4, C_{2v} (**4**)	b55, C_s (**5**)	b55′, C_2 (**6**)	v5, C_s (**7**)
661, e [4]	702 [13]	691 [9]	659 [8]	664 [6]	459 [17]	681 [6]	493 [14]	307 [42]
925, e [2]	840 [6]	804 [5]	661 [4]	689 [6]	528 [4]	782 [7]	671 [13]	510 [73]
1003, e [6]	915 [4]	917 [5]	824 [10]	737 [11]	549 [13]	813 [20]	736 [5]	639 [17]
1093, e [47]	1015 [6]	1015 [3]	941 [6]	795 [9]	580 [6]	828 [5]	811 [12]	707 [15]
1138 [21]	1051 [6]	1051 [7]	1050 [6]	957 [4]	613 [10]	853 [19]	915 [13]	747 [15]
	1063 [23]	1058 [13]	1078 [26]	1050 [3]	725 [16]	858 [6]	973 [4]	881 [22]
	1067 [16]	1068 [21]	1080 [24]	1066 [30]	870 [14]	923 [12]	1009 [6]	923 [27]
	1125 [11]	1115 [15]	1102 [12]	1086 [21]	933 [4]	984 [5]	1054 [5]	956 [13]
	1163 [8]	1137 [12]	1401 [3]	1115 [10]	1000 [7]	1083 [23]	1076 [22]	972 [13]
	1325 [8]	1440 [12]		1915 [10]	1035 [30]	1088 [46]	1082 [29]	981 [17]
	2144 [15]	2162 [15]			1059 [19]	1122 [7]	1119 [7]	1005 [24]
					1097 [23]	1841 [210]	2062 [36]	1008 [23]
					1213 [6]			1052 [56]
								1061 [18]
2629 [18]	2732 [82]	2730 [85]	2741 [38]	2717 [50]	2668 [25]	2740 [51]	2740 [75]	2726 [69]
2645, e [969]	2742 [85]	2741 [54]	2745 [43]	2737 [12]	2736 [178]	2744 [133]	2743 [23]	2733 [54]
2661 [923]	2743 [33]	2743 [50]	2746 [24]	2742 [108]	2739 [190]	2747 [46]	2747 [67]	2757 [191]
	2745 [45]	2744 [68]	2754 [284]	2744 [20]	2742 [45]	2759 [154]	2747 [107]	2769 [106]
	2750 [261]	2750 [221]	2759 [185]	2745 [117]	2775 [398]	2768 [191]	2756 [314]	2770 [152]
	2761 [277]	2761 [303]	2763 [65]	2755 [115]	2779 [358]	2781 [254]	2764 [14]	2773 [107]
	2780 [307]	2771 [189]	2771 [300]	2758 [5+8]	2781 [345]	2791 [37]	2767 [365]	2789 [397]
	2786 [196]	2782 [314]	2792 [328]	2766 [176]		2794 [167]	2779 [520]	2794 [325]
	2791 [126]	2794 [139]	2795 [177]	2775 [403]		2804 [278]		
	2808 [94]	2806 [89]	2805 [39]	2788 [28]		2817 [111]		

[a] Harmonic frequencies, cm^{-1}. [b] In brackets, kM/mol.

in $B_{10}H_{11}^{-}$ is situated over a triangular polar face and that it can migrate around the 4-fold axis with a small energy barrier.

The antipodal effect,[24] i.e. the sharp downfield shift of $\delta(^{11}B)$ of the "opposite" polar boron atom B10, in the $B_{10}H_{11}^{-}$ anion is noteworthy. The antipodal effect is especially large in B_9H_9X compounds (X = BH^{2-}, AlH^{2-}, CH^{-}, SiH^{-}, N^{-}, P^{-}, NH, PH, O, S).[23] The additional proton in $B_{10}H_{11}^{-}$ influences the chemical shift of the antipodal B10 atom (+17.9 ppm, IGLO; +25.7 ppm, experiment) to a similar extent as the exchange of the apical BH^{2-} group by a CH^{-} (+32.2 and +28.4 ppm).[23]

IR Frequencies. The experimental IR spectrum of $B_{10}H_{11}^{-}$ in the 2600–2800-cm^{-1} region (terminal BH bond vibrations) changed strongly[2] with respect to $B_{10}H_{10}^{2-}$. Many more signals appeared and were shifted to higher wavenumbers by 70–95 cm^{-1}. Similar changes were observed in going from $B_6H_6^{2-}$ to $B_6H_7^{-}$.[2] The calculated IR frequencies for $B_{10}H_{10}^{2-}$ and the various $B_{10}H_{11}^{-}$ forms (see Table IV) reproduce the experimentally observed trends. The shift of the terminal BH bond vibrational frequencies is computed to be about 100–140 cm^{-1}.

The most characteristic differences between the vibrational spectrum of $B_{10}H_{10}^{2-}$ and those of the various $B_{10}H_{11}^{-}$ structures are associated with the bridging hydrogen. In the t455 configuration **1**, the 2144-cm^{-1} vibration describes the movement of the triply bridging H* perpendicular to the B1B2B3 face plane. In the b45, b55, and b55′ structures with "normal" doubly bridging hydrogens, the characteristic frequencies are 1915, 1841, and 2062 cm^{-1}, respectively. One peculiarity of the IR spectrum of the triply bridged t555 configuration is the relatively small frequency of the B_5–H* stretching vibration, ca. 1400 cm^{-1}. The frequencies associated with the BH_2 group is the v4 form are 549 cm^{-1} (BH_2 rotation) and 1213 cm^{-1} (BH_2 bending). Unfortunately, the experimental $B_{10}H_{11}^{-}$ vibrational spectrum has not been published.

Conclusions

Both energetic and NMR evidence indicates that the additional hydrogen, H*, in the $B_{10}H_{11}^{-}$ anion is situated over a triangular face in the "polar region" near B1. In accord with the earlier calculations,[11] rotation around the 4-fold axis occurs with a small barrier (~2 kcal/mol). However, the transfer of the extra hydrogen from one polyhedron pole to the other is calculated to have a high barrier (~19 kcal/mol); the experimental value is somewhat lower (13 ± 1.5 kcal/mol). A structural feature of the global $B_{10}H_{11}^{-}$ minimum is the marked extension (to 2.00 Å) of one of the basal BB bonds connected to the additional proton. However, a weak bonding interaction between these boron atoms is indicated by a significant overlap population. Therefore, the closo structure of $B_{10}H_{10}^{2-}$ is not fully transformed into a nido form upon protonation.

Acknowledgment. This work was supported jointly by the Deutsche Forschungsgemeinschaft and the Russian Academy of Sciences, as well as by the Fonds der Chemischen Industrie, the Stiftung Volkswagen-werk, and the Convex Computer Corp. The calculations were performed on a Convex-C220 computer of the Institut für Organische Chemie and on a Cray Y-MP4 computer of the Leibniz Rechenzentrum Munich. We thank Professor W. Kutzelnigg and Dr. M. Schindler for the Convex version of the IGLO program which is available for distribution. A.M.M. thanks all members of the theoretical group of the Institut für Organische Chemie and Dr. N. v. E. Hommes and Dr. A. S. Zyubin especially for helpful advice.

(24) (a) Plesek, J.; Hermanek, S. *J. Chem. Soc., Chem. Commun.* **1975**, 127. (b) Todd, I. J.; Siedle, A. R.; Bodner, G. M.; Kahl, S. B.; Hicke, J. P. *J. Magn. Reson.* **1976**, *23*, 301. (c) Leyden, R. N.; Sullivan, B. P.; Baker, R. T.; Hawthorne, M. F. *J. Am. Chem. Soc.* **1978**, *100*, 3758. (d) Teixidor, F.; Vinas, C.; Rudolph, R. W. *Inorg. Chem.* **1990**, *25*, 3339.